A Climatology-Based Forecast Tool for Coastal Flooding in the Low Country

JOSEPH COZ,[a] FRANK ALSHEIMER,[b] AND BERNHARD LEE LINDNER[a]

[a] *College of Charleston, Charleston, South Carolina*
[b] *NOAA/NWS/Weather Forecast Office, Columbia, South Carolina*

(Manuscript received 5 November 2020, in final form 17 April 2021)

ABSTRACT: Coastal nuisance flooding has increased by an order of magnitude over the past half century, but the National Weather Service has a limited suite of statistical tools to forecast it. Such a tool was developed using coastal flood events from 1996 to 2014 in Charleston, South Carolina, that were identified and classified by prevailing synoptic conditions based on composite mean sea level pressure anomalies. The synoptic climatology indicated low-level northeasterly winds dominated the forcing in anticyclonic and cyclonic events, while a southeasterly surge was the main forcing component for frontal events. Tidal anomalies between flood events and previous low tides were used to create linear regression models for each composite classification studied for forecasting levels of coastal flood magnitude. Beta tests using data from 2018 to 2019 confirmed the effectiveness of the models with RMSE values less than 0.3 ft (9 cm) and MAE values less than 0.25 ft (7.6 cm) for each event type. The veracity of the methods was further verified by a multiple-day case study from November 2018, where the model was tested against both statistically predicted heights and heights based on the NOAA extratropical storm surge (ETSS) model (version 2.2). The RMSE and MAE for the statistical model were 0.18 and 0.15, respectively, while the same values for the ETSS model were 0.28 and 0.23, respectively.

SIGNIFICANCE STATEMENT: Nuisance coastal flooding in Charleston, South Carolina, occurs numerous times per year and causes disturbances in traffic, commerce (financially and socially), and human health. Charleston has spent hundreds of millions of dollars (and counting) on drainage projects and seawall raisings. Furthermore, flooding has caused gross damages and lost wages of nearly $2 billion. As global sea levels continue to rise, the annual number of coastal flooding events in Charleston continues to increase. This climatology-based forecast tool will aid forecasters in the accurate prediction of tides that cause the inundation in the Charleston area as well as support the timely issuance of coastal flood advisories, watches, and warnings to help protect life and property.

KEYWORDS: Climatology; Coastal meteorology; Forecasting; Forecasting techniques; Operational forecasting; Flood events; Sea level

1. Introduction

A flood is an overflowing of an amount of water beyond its normal confines, especially over what is normally dry land (Kriebel and Geiman 2014). Some areas are more prone to flooding than others, and there are multiple different types of flooding that can occur. A coastal flood is the inundation of land areas along the coast as a result of a higher-than-average high tide (Dahl et al. 2017). Coastal floods range from nuisance-level events to severe storm surges caused by tropical cyclones, and they can be worsened by heavy rainfall or onshore winds (Moftakhari et al. 2015). Chronic coastal flooding can have a variety of negative environmental, economic, and social end points (Gornitz et al. 1994; Curtis et al. 2004; Nicholls 2004; Adger et al. 2005; Moftakhari et al. 2015; Behre 2017; Behre and Darlington 2017).

Coastal communities in the U.S. Southeast are at high risk for inundation or increased erosion from sea level rise due to their characteristics, which include subtropical climate, low coastal elevations, erodible substrates, present and past evidence of subsidence, histories of extensive shoreline retreat, high wave/tide energies, and high probabilities of experiencing landfalling tropical cyclones (Gornitz et al. 1994; McLean et al. 2001; Spanger-Siegfried et al. 2014; Sweet et al. 2014). Charleston, South Carolina, and the South Carolina coastline are no exception to this statement (Alsheimer and Lindner 2011; Lindner and Neuhauser 2018). The historic core of the city of Charleston is a peninsula surrounded by the Charleston Harbor on three sides, and it is located just southwest of the geographic midpoint of South Carolina's coastline (Fig. 1). Its proximity to the Atlantic Ocean allows the threat of both coastal flooding and, in more severe cases, storm surge (especially from tropical cyclones). Furthermore, the Charleston Harbor is an inlet of the Atlantic Ocean formed by the confluence of the Ashley, Cooper, Wando, and Stono Rivers (Fig. 1), making the city and the surrounding areas susceptible to the impacts of river floods, as well as flash floods from intense rainfall.

Although Charleston is prone to all types of flooding, it is most frequently impacted by the effects of nuisance coastal flooding, which can be exacerbated by coincident heavy rainfall. In Charleston, such flooding occurs when water levels exceed 7 ft above mean lower low water (MLLW; City of Charleston 2015; NOAA 2020a; 1 ft ≈ 0.305 m). Unfortunately, tides observed above this threshold have become an increasingly common phenomenon as sea levels have gradually risen during the last half century as a

Corresponding author: Joseph Coz, joeycoz@gmail.com

DOI: 10.1175/JAMC-D-20-0256.1

FIG. 1. This is a map of the Charleston Harbor watershed, including the Ashley, Cooper, Wando, and Stono Rivers. It was created by Karl Musser based on USGS and U.S. Census Bureau data. The tide station that collected all the tide level data used in this research is represented by a black star on the peninsula or Charleston.

result of global climate change (Smith and Ward 1998; Nicholls and Cazenave 2010; IPCC 2013; Sweet et al. 2014; Moftakhari et al. 2015; Dahl et al. 2017). A 3.4 mm yr^{-1} rise in sea level is attributed to the combination of thermal expansion of seawater and melting of glaciers and ice sheets (Lindsey 2020), and the global sea level has risen by over 210 mm since 1880 (Church and White 2011). Significant areas of the U.S. coastline could be permanently inundated by the end of the current century (Walsh et al. 2014).

Coastal flooding along the East, Gulf, and West Coasts occurred approximately once every 3 months by the year 2012 but was only occurring every 1–5 years during the 1950s (Sweet et al. 2014). The rising trend in coastal flood events can be seen in Fig. 2, evident even above interannual variability and noise. Charleston may see as many as 200 or more flood events per year by 2045 (Dahl et al. 2017).

The National Weather Service (NWS) recognizes coastal flood severity with three categories, and each category is defined according to the property damage and public threat it poses. The first category is minor flooding, which is defined by minimal or no property damage but possibly some public threat or inconvenience (Gornitz et al. 2001; NWS 2018, 2019a). Generally, the inundation during a minor coastal flood is 1 ft or less (NWS 2018). Minor coastal flooding is commonly referred to as ''nuisance flooding'' because of the inconveniences and annoyances it causes to the daily lives of citizens, tourists, businesses, traffic patterns, and public officials (Gornitz et al. 2001; Dahl et al. 2017). Such flooding events are caused by short-term sea level rise resulting from strong cyclones, strong anticyclones, wind surges, and frontal heads (Sweet et al. 2009; Wolf 2009; Woodworth et al. 2014). Although there may be minimal to no direct risks to life, these coastal flooding events repeatedly impact the lowest lying areas. This repetitive inundation can lead to negative health end points (Curtis et al. 2004) as well as property destruction from redundant inundation. Furthermore, it creates negative financial impacts on business and commerce due to frequent road closures (City of Charleston 2015). In Charleston, however, when a minor coastal flooding event is coupled with a severe or persistent rainstorm, some streets will become inundated to the point where they are impassable and any parked cars in these areas would need to be moved to higher ground. It is not uncommon for building entrances in low-lying areas to have to be sandbagged to keep water from entering the building.

The second coastal flood severity category recognized by the NWS is moderate flooding. Moderate flooding occurs when there is some inundation of vulnerable structures and roads, but widespread damage or evacuations do not take place (NWS 2018). The causes of such flooding are more often than not the same as those for minor coastal flooding. However, the level of inundation is greater—generally 1–2 ft (NWS 2018).

The third category is severe (or major) coastal flooding. During these events, the inundation level is generally between 2 and 4 ft, which results in extensive inundation of structures and roads and significant evacuations of people and/or transfer of property to higher elevations (NWS 2018). Coastal flooding events in Charleston typically only reached major severity levels in the past when a tropical cyclone or an unusually strong extratropical cyclone effected the area, however, reaching these levels has become more common in the past 20 years, with the existence of a strong cyclone no longer a requirement for implicating severity.

The NWS also uses a three-tiered watch–warning–advisory system to communicate the potential threats and impacts of coastal flooding events (NWS 2020). In Charleston, a coastal flood watch is typically issued 12–48 h in advance when there is a possibility of the water levels reaching or exceeding 8 ft above MLLW. A coastal flood warning is issued when the water level is likely to reach or exceed 8 ft above MLLW in the next 12–24 h (NWS 2020). A coastal flood advisory is typically issued in when the water level is expected to reach or exceed 7 ft above MLLW but remain less than 8 ft above MLLW, in the next 6–12 h. (NWS 2020). Such events are defined in this paper as nuisance coastal flooding. Water levels below 7 ft MLLW do not have meaningful impacts.

Events that require the issuance of a coastal flood advisory can be difficult to predict (Gornitz et al. 2001; Nicholls 2004). Often, the predictions of such events are based on correlations between water levels at a tide gauge and reported instances of observed flooding. These predictions are often based on observational data rather than statistical simulations (Dahl et al. 2017). Because the current number of statistical tools available for predicting nuisance-level coastal floods is limited, it is imperative that the NWS offices develop new models for improved prediction of such events. Furthermore, the atmospheric drivers of coastal nuisance flooding in the South Atlantic Bight are not as well understood as they are in the mid-Atlantic states (Sheridan et al. 2017).

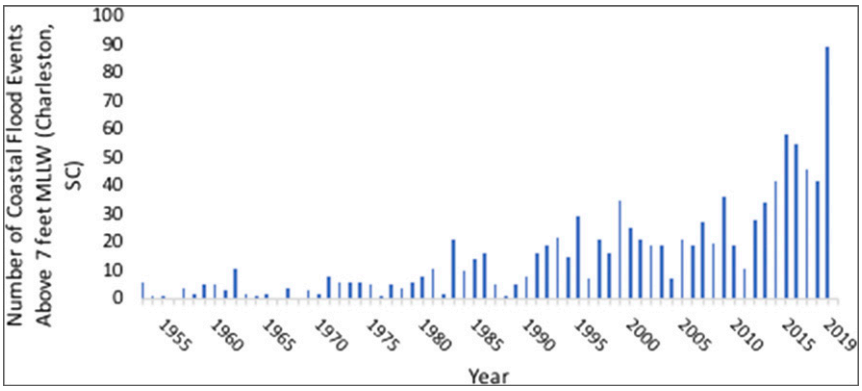

FIG. 2. The number of events per year from 1953 to 2019 where the tide level reached exceeded 7 ft above MLLW. This figure was generated from the NWS's Coastal Flood Event Data Base for Charleston.

As mentioned earlier, nuisance flooding events pose limited direct risks. However, they are accompanied by several indirect risks such as power outages, heavy traffic, and backing up of storm drains and sewers (Colle et al. 2010; Spanger-Siegfried et al. 2014; Sweet et al. 2014; City of Charleston 2015, 2019a). Although such events do not require evacuation, there are numerous short-term mitigation efforts that must be employed, such as temporary road barriers and the sandbagging building entrances. While the impacts of nuisance coastal flooding in the Charleston area are currently considered "minor," they begin to take on a new level of significance as their occurrences become more chronic. It is imperative for coastal communities to assess vulnerability and implement plans to mitigate the impacts of coastal flooding (Gornitz et al. 1994; McLean et al. 2001; Adger et al. 2005). Many communities are unprepared to deal with the weekly to daily occurrences of coastal flooding (Spanger-Siegfried et al. 2014), while some communities are working toward developing policies and building infrastructure to adapt to this unprecedented challenge.

Charleston is actively taking the necessary and costly steps to address the ecological, social, and economic impacts of coastal flooding. It has been calculated that the city has spent $239 million on drainage projects and pump stations since 1984 (Behre and Darlington 2017; Slade 2017). The city has also determined that the battery seawall on the southernmost edge of the peninsula will need to be raised at least 2.5 ft to combat the impacts of sea level rise and coastal flooding. The raising of this mile-long wall is expected to cost over $100 million and take more than a decade to complete (Behre 2017).

There are two main goals to this study. The first is to better understand the atmospheric patterns that lead to nuisance coastal flood events specifically in the Charleston vicinity. The second is to derive a climatologically based statistical tool to help determine the extent of nuisance flooding expected at a given high tide based on data from the previous low tide. While the study focuses on providing the forecasters of the NWS office in Charleston (CHS) with a model for doing so, the methodology used to create that model can be applied to locations worldwide. The synoptic climatology will provide CHS forecasters with up to a 48-h lead time of the potential for nuisance flooding events, promoting general awareness. The statistical tool, in the form of scatterplots and regression equations will help refine the range of potential water height forecasts within 6 h of the actual event. This allows for appropriate short-term mitigation actions, such as road closures, sandbagging, and transportation route alterations, to be taken to protect property and infrastructure before inundation begins (City of Charleston 2019b; Charleston County Government 2021).

2. Methods

The study site for this project is Charleston and the study period includes the years from 1996 to 2014. A period of 19 years was chosen to match the length of a tidal epoch, as defined by NOAA (NOAA 2020a). All tide cycles during these years were analyzed in detail to identify the events where the actual observed water levels exceeded the coastal flood threshold of 7 ft above MLLW. The weather maps created from this datum provide the forecasters with synoptic climatology of the current meteorology that influences nuisance coastal flooding, and the scatterplots provide additional forecast guidance. The locations of the tide station used to collect tide data in Charleston is represented in Fig. 1. The site of the tide station was established in 1899, and the present instrumentation was installed in 1990 (NOAA 2020b). Figure 3 provides photographs of the station.

a. Retrieval of historic tidal readings

Historical 6-min tidal data for Charleston were downloaded from NOAA's Tides and Currents website (NOAA 2020b) for the years 1996–2014. These data allow for the observation of actual tide gauge readings and astronomically predicted tide values at 6-min intervals. These data tables were analyzed and all instances where observed water levels were equal to or greater than 7 ft above MLLW were identified. For tide cycles when multiple consecutive 6-min observations of $\geq$7 ft above MLLW were recorded, the peak water level at that single tide cycle was identified. Furthermore, the corresponding previous low tide event was recorded. Often these values would fall below the MLLW.

FIG. 3. Photographs of the tide station 8665530 Charleston, Cooper River entrance (NOAA 2020b).

b. Determine climatological anomalies for flood tides

The tidal anomaly can be defined as the difference of the observed water level and the astronomically predicted water level. To create the necessary scatterplots for providing forecasters with accurate 6-h lead times, anomaly values are needed for both the flood tide event and the previous corresponding low tide event. The term ''delta high'' is used to represent the difference between the astronomically predicted high tide and the actual verified high tide. The term delta low is used to represent the difference between the astronomically predicted low tide and the actual verified low tide that preceded. For example, at 0530 eastern standard time (EST) 5 December 2014, there was a predicted low tide of 0.588 ft below MLLW. However, the actual low tide was verified at 0.543 ft above MLLW. The difference of these two values, 1.131, is the delta low. Delta high is calculated the same way but using the values of the high tide.

c. Separation of events into type-based categories

After establishing the dates and approximate times of every flood tide event, mean sea level pressure anomalies were determined from maps created using the 6-h NCEP–NCAR reanalysis data composite available from NOAA's Earth System Research Laboratory (ESRL). The domain for the study was 20°–50°N, 60°–90°W to identify atmospheric pressure systems that were most likely to have a direct influence on tidal levels in Charleston through atmospheric–oceanic feedback processes. The mean sea level pressure anomaly weather maps were then classified into one of five synoptic categories: anticyclonic, cyclonic, frontal, neutral, and tropical. While there were times that multiple features might be captured within the domain defined above, specific criteria were used based on mean sea level pressure (MSLP) anomalies to determine the dominant type for the event category. Anticyclonic events were identified when maximum absolute value of positive anomalies (when MSLP values are greater than the climatological mean) within the domain was more than 2 hPa greater than the maximum absolute value of the negative anomalies (when MSLP values are less than the climatological mean) (Fig. 4a). Cyclonic events were identified when the maximum absolute value of negative anomalies within the domain was more than 2 hPa greater than the maximum absolute value of the positive anomalies (Fig. 4b). Neutral events were identified when the difference of maximum and minimum anomaly absolute values were 2 hPa or less, indicating no dominance of either cyclonic or anticyclonic systems within the domain (Fig. 4c). Frontal events were identified by a front passing through or within 50 n mi (1 n mi = 1.852 km) of Charleston Harbor, based on the NOAA/NWS Daily Weather Maps (Fig. 4d) (NOAA 2018). Events were classified as tropical cyclones if they passed within 100 n mi of Charleston, based on HURDAT2 Best Track Data. (Landsea and Franklin 2013) (Fig. 4e). Such events only accounted for 9% of the flooding events that occurred during the study period and were removed from the study because additional model-based tools, which are specifically tuned to

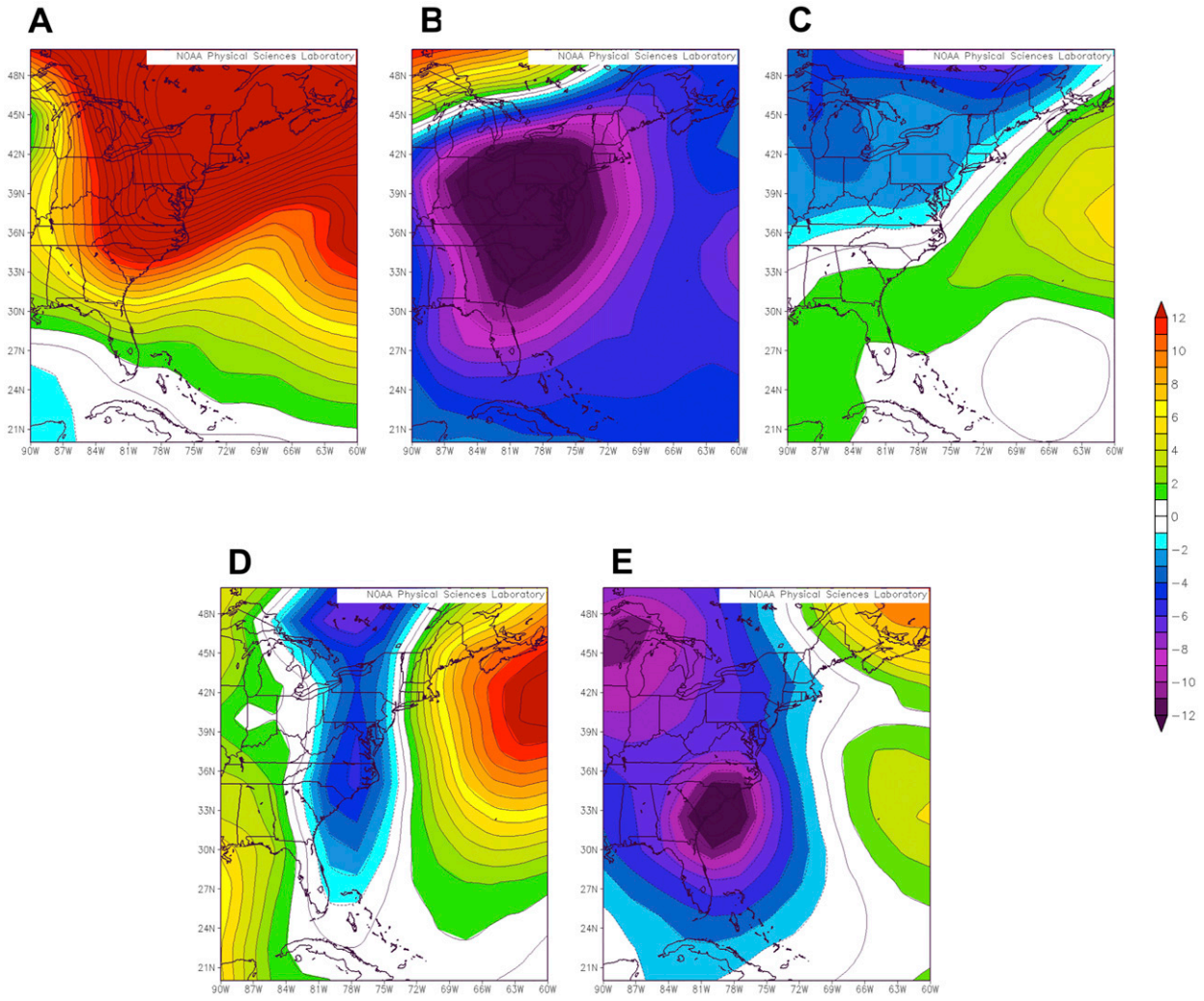

FIG. 4. Examples of the five different synoptic categories. (a) Anticyclonic events have a maximum absolute value of positive anomalies within the domain more than 2 hPa greater than the maximum absolute value of the negative anomalies. (b) Cyclonic events have a maximum absolute value of negative anomalies within the domain more than 2 hPa greater than the maximum absolute value of positive anomalies. (c) Events are identified as neutral when the difference of maximum and minimum anomaly absolute values are 2 hPa or less. (d) Frontal events were identified by a front passing through or within 50 n mi of Charleston Harbor. (e) Tropical events are identified as events where a tropical cyclone passes within 100 n mi of Charleston.

tropical cyclones are available to forecasters for these events (Alsheimer and Lindner 2011).

Composite mean and composite mean anomaly weather maps were created for each event type using NOAA/ESRL data. These composite maps were produced for geopotential height, air temperature, and vector wind at 925, 850, 700, 500, and 300 hPa, as well as for sea level pressure and vector wind at the surface. Maps were produced for day of event (d), 1 day prior to event ($d - 1$), and 2 days prior to event ($d - 2$).

d. *Classifying consecutive flooding events into one date and time*

Many of the events where the actual water level exceeded 7 ft above MLLW occurred over the course of 2 or more consecutive days. Mean sea level pressure anomaly maps were used to determine if these consecutive events were the result of the same single synoptic influence. In such cases, the day and time with the greatest delta high was selected to represent the event. For example, the coastal flooding threshold was breached during both daily tide cycles on 27–28 February 1998. These four events were confirmed to have been under the same meteorological influences. The greatest delta high was observed on 1330 EST (0054 UTC) 27 February 1998.

e. *Delta high versus delta low scatterplots*

After the events were separated into synoptic categories, the tropical cyclone data were removed, and the consecutive flood events were all represented by one date and time, scatterplots were created for each of the synoptic categories. Delta low was used as the independent variable (x axis) and delta high as the

dependent variable (y axis). The linear regression equation presented in the scatterplots gives forecasters approximately a 6-h lead time to forecast flood tides based on previous low tides. Delta low is simply the difference between the observed and astronomically predicted low tide. Once the forecaster has access to the observed low tide value, they can calculate delta low and enter it into the equation to output a delta high value. This delta high value can then be added to the upcoming astronomically predicted high tide to create a value that more accurately represents the level of the upcoming high tide.

f. Identification of outliers

During regression analysis, outliers are identified by analyzing the residuals for each event. The residual (e) can be defined as the difference between the observed value of the dependent variable (y) and the predicted value ($\hat{y}$). Events where the absolute value of the residual is greater than 2 are defined as large and can be identified as outliers.

The dates and times of outlier events were noted, and weather maps were created using the 6-h NCEP–NCAR reanalysis data composite available from NOAA/ESRL. Composite mean anomaly maps were produced at time of event, 6 h before event, 12 h before event, 18 h before event, and 24 h before event for geopotential height, air temperature, and vector wind at 925 and 850 hPa for each outlier event. The maps were analyzed to determine what made these events unique. The identification of outliers will also give forecasters examples where the forecast tools would have trouble producing accurate predictions.

g. Independent data analysis

Historical 6-min tidal data for Charleston were downloaded from NOAA's Tides and Currents website (NOAA 2020b) for 2018–19. The data were analyzed for instances of actual water levels equal to or greater than 7 ft above MLLW, along with the corresponding previous low tide. Each event was assigned one of the four synoptic categories and scatterplots were created for each category. The trendlines created from the 1996–2014 data were superimposed over the scatterplots for a visual analysis of how well the model held true during 2018–19. Statistical significance was determined by calculating the root-mean-square error (RMSE) and mean absolute error (MAE) values for the independent 2018–19 data.

3. Results

There were 368 nontropical tidal events identified that exceeded the nuisance flooding threshold (7 ft above MLLW) over the course of the 19-yr epoch. Each event was assigned a category by analyzing the sea level pressure during the date and time of the flood tide. Instances where the observed flood tide exceeded 7 ft above MLLW over the course of multiple consecutive days from the same meteorological cause were combined and represented as one event. The total number of events decreased from 368 to 196 and of those events, 68 were anticyclonic (34.5%), 63 were cyclonic (32.0%), 36 were neutral (18.3%), and 29 were frontal (14.7%). The years with the fewest and most nuisance coastal flooding events were 2004 and 2014, respectively.

a. Anticyclonic events

Anticyclonic event composite means for surface level pressure are shown in Fig. 5a. Two days prior to the maximum tidal level ($d - 2$) the composite surface analysis map shows a general area of higher pressure in the eastern Great Lakes and Ontario, with a trough or front located in the western Atlantic Ocean offshore of the eastern United States. One day closer to the event ($d - 1$), the signal is strengthening as it moves southeastward to a position centered over central Pennsylvania. The composite map for the event days (d) shows a continued consolidation as the highest pressures move toward the New York–New Jersey area, including the adjacent coastal waters with a ridge of higher pressure extending down the entire East Coast of the United States. The composite mean anomalies for sea level pressure show that anticyclonic events are dominated by higher-than-normal pressure across the entire eastern third of the United States, relative to nonflood events (Fig. 6).

Anticyclonic event composite means for vector wind speed at the surface are presented in Fig. 7a. Even at $d - 2$, stronger northeasterly winds than average are evident in the North Atlantic Bight, indicating wind forcing is already driving some water toward the coast in advance of the event days. By $d - 1$, there is noticeably stronger northeasterly winds off the Delmarva coast. By the event day, the northeasterly winds extend from the western Atlantic Ocean to the coastline of the Carolinas and Georgia. This flow runs parallel to the South Carolina coastline and transports water toward the coast via the Ekman effect (Sverdrup et al. 1942).

b. Cyclonic events

Cyclonic event composite means for atmospheric pressure at the surface are presented in Fig. 5b. On $d - 2$, the composite surface analysis map shows a general area of low pressure in the Atlantic Ocean off the coast of the mid-Atlantic states. One day closer to the event, the initial area of lower pressure moves farther north and out into the Atlantic Ocean. However, a new area of lower pressures has shown up in the southeastern Gulf of Mexico, stretching across Florida and the Bahamas. By the day of the event, deeper low pressure has consolidated in the western Atlantic Ocean, with lowest values extending from the Florida east coast to the Atlantic offshore of South Carolina.

This set of composite maps indicates a typical scenario for low pressure development in the region. An initial area of low pressure in the western Atlantic Ocean has a cold front that trails southwestward across Florida into the southern Gulf of Mexico. As the low pressure area in the Atlantic moves away, a new area of low pressure begins to form along the trailing front across the eastern Gulf of Mexico. By the end of the event, the low has moved into a favorable position offshore of South Carolina and Georgia. This pressure pattern implies a strengthening of onshore flow along the South Carolina coastline.

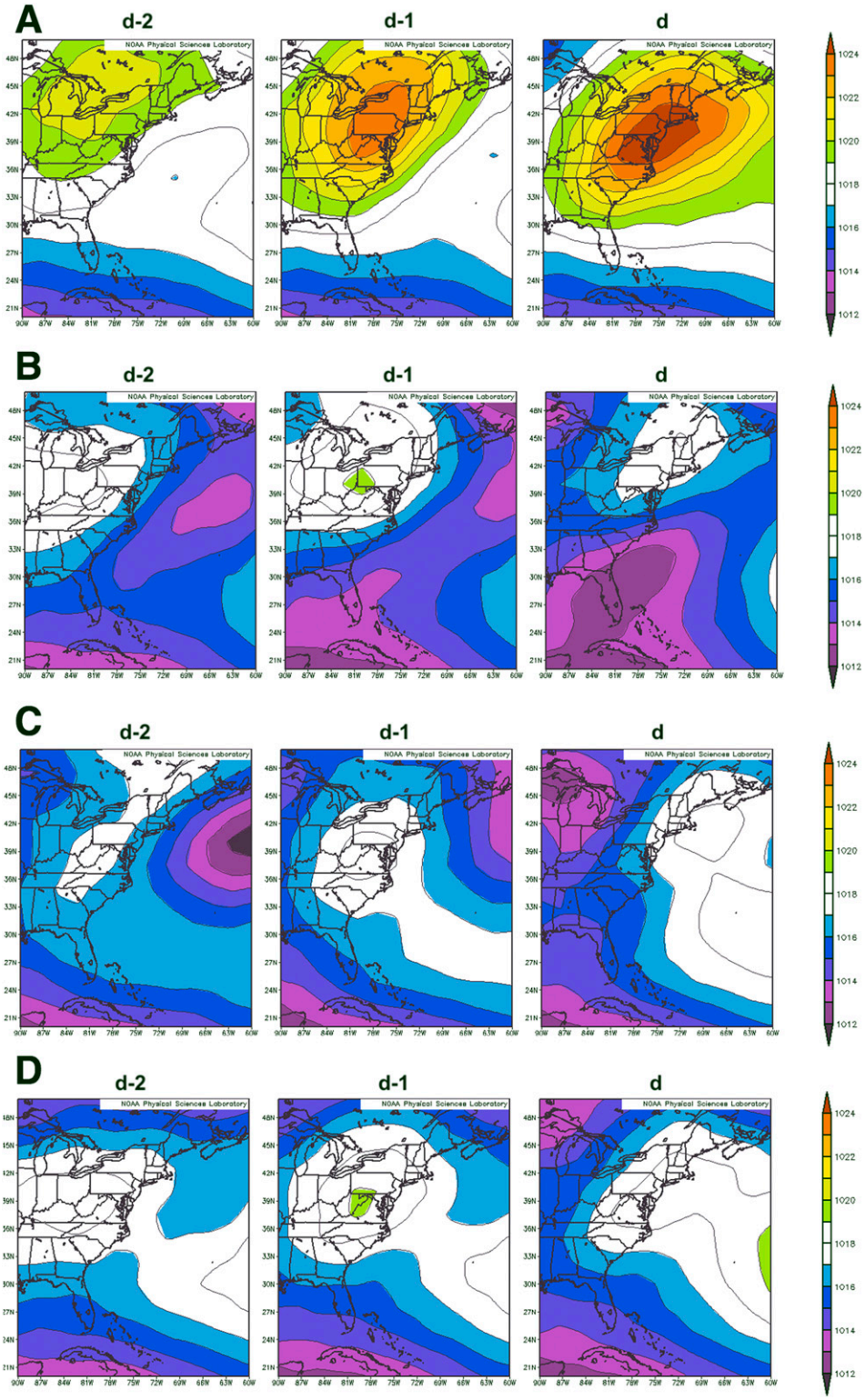

FIG. 5. (a) 3-day NCEP–NCAR reanalysis plots for anticyclonic event composite means for sea level pressure at the surface. Sea level pressure is measured in hectopascals (hPa). (b) 3-day NCEP–NCAR reanalysis plots for cyclonic event composite means for sea level pressure at the surface. (c) 3-day NCEP–NCAR reanalysis plots for frontal event composite means for sea level pressure at the surface. (d) 3-day NCEP–NCAR reanalysis plots for neutral event composite means for sea level pressure at the surface. For each panel, d represents day of, $d - 1$ represents 1 day prior, and $d - 2$ represents 2 days prior and sea level pressure is measured in hectopascals (hPa).

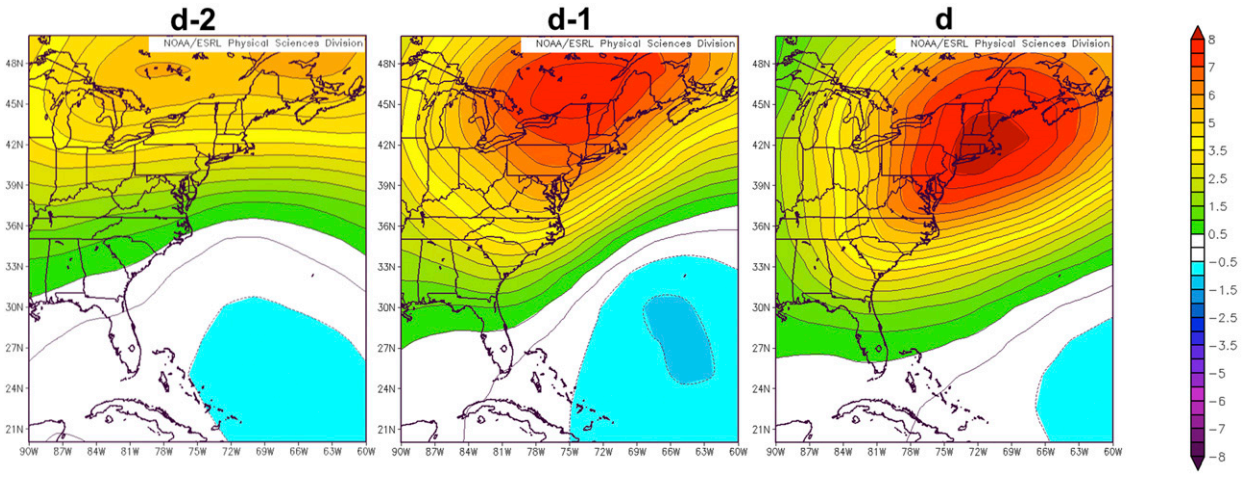

FIG. 6. 3-day NCEP–NCAR reanalysis plots for anticyclonic event composite mean anomalies for sea level pressure at the surface. Sea level pressure anomalies are measured in hectopascals (hPa), and d represents the day of, $d-1$ represents 1 day prior, and $d-2$ represents 2 days prior.

Cyclonic event composite means for vector wind speed at the surface are presented in Fig. 7b. Stronger than normal northeasterly winds are occurring throughout the days leading to the events. At $d-2$, this signal is strongest off the coast of the northeastern states. By the day before the events, the stronger northeasterly winds have increased in area, stretching along the coast from Cape Cod to South Carolina, including the adjacent Atlantic Ocean. While the location of the strongest winds is similar to the anticyclonic events (Fig. 7a), the magnitude of the winds is lower.

c. *Frontal events*

Frontal event composite means for sea level pressure and surface vector winds are shown in Figs. 5c and 7c, respectively. Together, these two panels tell the story of the wind water push toward the coast of South Carolina for the frontal events. On $d-2$, the composite mean surface analysis map is dominated by lower pressure in the North Atlantic to the south of Nova Scotia. A small maximum in the composite sea level pressure follows behind the lower pressure into the mid-Atlantic by $d-1$, but quickly moves into the Atlantic Ocean as lower pressures approach from the west on the day of the event in association with a front. The vector wind means show little in the mean on $d-2$ near South Carolina, indicating weak high pressure in the southeastern United States, but do indicate low pressure in the North Atlantic south of Nova Scotia. However, the first signs of return flow show in the South Atlantic Bight by $d-1$ as the mean center of the high moves offshore into the Atlantic Ocean and surface winds gain an easterly component. By the day of the events the mean winds are out of the south and southeast and increasing in magnitude ahead of the approaching front.

d. *Neutral events*

The neutral event composite mean maps for sea level pressure at the surface are shown in Fig. 5d, and the neutral event composite mean anomaly maps for vector wind at the surface are shown in Fig. 7d. The neutral event composite map panels reflect this definition and share similarities with the cyclonic and anticyclonic events as northeasterly flow gradually increase off the southeast coast of the United States, but the magnitudes are much weaker than the other categories. The general low magnitudes of both the mean and the anomaly (not shown) values make neutral event flooding more difficult to predict. This suggests that tide levels could be affected by factors that are not identified by the parameters used in this study.

e. *Scatterplots*

Scatterplots were created for each synoptic category with delta low on the x axis and delta high on the y axis (Fig. 8). Once the threat for a nuisance (or greater) coastal flood event has been identified by forecasters, the scatterplots will provide a reasonable range of expected values within 6 h of the event for response purposes. After the low tide and delta low have been observed, forecasters can then use the best-fit line to project the most likely value of the high tide (delta high plus astronomically predicted high tide) based on the study. They can also use the confidence intervals for the resulting linear regression to project a likely range of values.

f. *Outlier events*

The fits and diagnostics test for unusual observations produced four anticyclonic observations, three cyclonic observations, zero frontal observation, and zero neutral observation that had large residual values. As defined in the methods, observations where the absolute value of the residual is greater than 2 are defined as large and can be identified as outliers. The dates, times, and delta values for these observations are represented by Table 1.

For anticyclonic events, outliers generally fell into one of two categories. First, situations where synoptic features moved faster than usual so that the mean anomalies did not represent the atmospheric forcing scenario well. An example of this

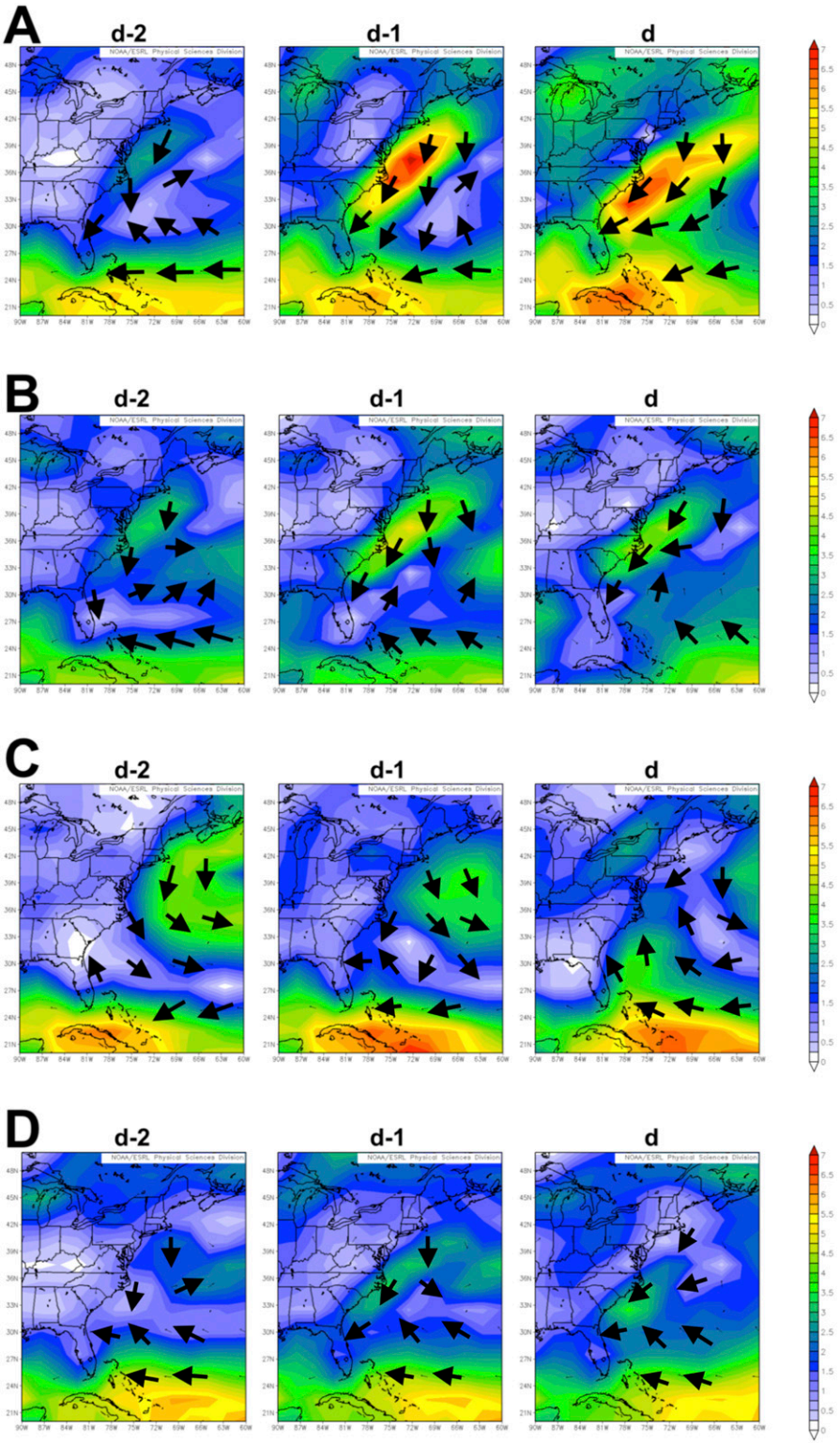

FIG. 7. (a) 3-day NCEP–NCAR reanalysis plots for anticyclonic event vector wind composite means at the surface. (b) 3-day NCEP–NCAR reanalysis plots for cyclonic event vector wind composite means at the surface. (c) 3-day NCEP–NCAR reanalysis plots for frontal event vector wind composite means at the surface. (d) 3-day NCEP–NCAR reanalysis plots for neutral event vector wind composite means at the surface. For each panel, d represents the day of, $d - 1$ represents 1 day prior, and $d - 2$ represents 2 days prior. The wind speed means are measured in meters per second, and the wind direction is indicated by the arrows.

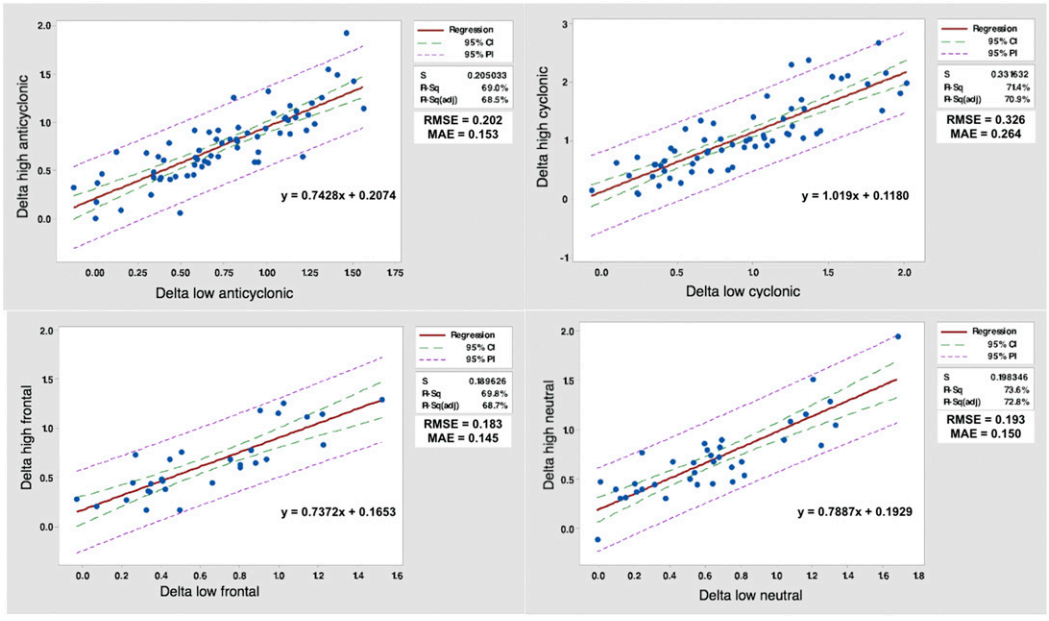

FIG. 8. Scatterplots for delta high vs delta low for each event type. Best-fit lines, confidence intervals, prediction intervals, linear regression equations, RMSE values, and MAE values are presented for each plot. The linear regression equation presented in the scatterplots gives forecasters approximately a 6-h lead time to forecast flood tides based on previous low tides. Delta low is simply the difference between the observed and astronomically predicted low tide. Once the forecaster has access to the observed low tide value, they can calculate delta low and plug it into the equation to output a delta high value. This delta high value can then be added to the upcoming astronomically predicted high tide to create a value that more accurately represents the level of the upcoming high tide.

occurred in May 1997, with high pressure in northern Canada moving all the way to the mid-Atlantic in 24 h, wind anomalies significantly increasing within 6–12 h. The other category included events that, while anticyclonically dominated based on the parameters of the study, also had the contributing factor of a large cyclone (either tropical or extratropical) in the far eastern portion of the domain, potentially enhancing Ekman transport (Yin et al. 2020).

Cyclonic event outliers contained a couple of systems that had very recently transitioned from tropical to extratropical, so the flood event was likely still being influenced by some tropical processes that were not meant to be captured in the study. Another outlier was a very rapidly deepening extratropical cyclone, with surface pressures dropping 8 hPa in less than 6 h.

4. Independent analysis

To test the viability of the dataset for future operations, flood events that occurred during 2018 and 2019 were examined as an independent analysis. There were 36 flood events identified for 2018 and 73 for 2019, for a total of 109 flood events during these two years. Out of the total 109 events during this period, 50 were categorized as anticyclonic, 20 as cyclonic, 15 as frontal, and 24 as neutral. Note that during the study period (1996–2014) there were a total of 196 flood events identified, so the frequency of events increased considerably in recent years.

The scatterplots for 2018 and 2019 are presented in Fig. 9. The trendlines from the 1996–2014 models have been superimposed over each scatterplot for a visual representation of how well the model works. To determine statistical significance for each model, RMSE and MAE values were calculated for each event type. These values are indicated on the scatterplots.

5. Case study (November 2018)

To check the veracity of the climatological method presented in the paper, the multiday coastal flooding event in late November of 2018 is examined. This case is shown as an example of the benefits of the method for operational forecasters.

On the morning of 24 November 2018, Charleston experienced its sixth highest tide on record, which measured 8.76 ft above MLLW (more than 2 ft above the astronomically predicted tide level of 6.67 ft MLLW). This tide exceeded the levels observed previously during many significant and well-known events, such as Hurricane David (1979) and the October 2015 storm (Hebert 1980; NWS 2016). Coastal flooding, as defined by MLLW reaching 7 ft or higher, also occurred during four other tidal cycles in the 4-day period from 22 to 25 November 2018 (Table 2).

To anticipate the potential for the flood event, operational forecasters would use numerical models to predict the expected sea level pressure pattern, including anomalies, to

TABLE 1. Dates, times, and delta values of the outliers identified by the fits and diagnostic test for unusual observations.

Date	Time (EST)	Delta high (ft)	Delta low (ft)	Event category
28 May 1997	0106	1.256	0.806	Anticyclonic
7 Oct 1998	1354	0.058	0.493	Anticyclonic
20 Mar 2000	0754	1.919	1.462	Anticyclonic
12 Sep 2006	1248	0.643	1.208	Anticyclonic
8 Oct 1996	0506	2.659	1.831	Cyclonic
27 Feb 2005	2218	2.364	1.369	Cyclonic
3 Jun 2007	0300	2.294	1.254	Cyclonic

determine the class of event that could take place. As early as 20 November 2018, while there was an area of low pressure (cyclone) south of New England at that time (Fig. 10), forecast models predicted an area of high pressure (anticyclone) to build over the northeastern United States by 23–24 November 2018, corresponding to the dates of the highest astronomically predicted tide close to 7 ft above MLLW. Based on the anticipated evolution, the case would fall into the anticyclonic category.

Daily surface vector wind maps for 20–25 November 2018 are presented in Fig. 11. These maps show similarities to the anticyclonic vector wind mean maps created in the synoptic climatology for the first several days. From 22 to 23 November 2018, the strengthening of the northeast winds is observed very similarly to how it developed in the synoptic climatology. The day leading up to the maximum flood event the northeast wind is moderate, and then on the day of the maximum flood event the winds quite strong. As discussed earlier, these northeast winds run parallel to the South Carolina coastline and transport water toward the coast via the Ekman effect. By 24 November, the case starts to look a bit more frontal with the winds becoming more southeast offshore of South Carolina, which would push the water farther onshore in the South Atlantic Bight region. Not surprisingly, the highest tide of the event occurred on that day (Table 2).

The regression model gives a lead time of approximately 6-h and produces reliable projections useful to the forecasting community. However, to check the value of this

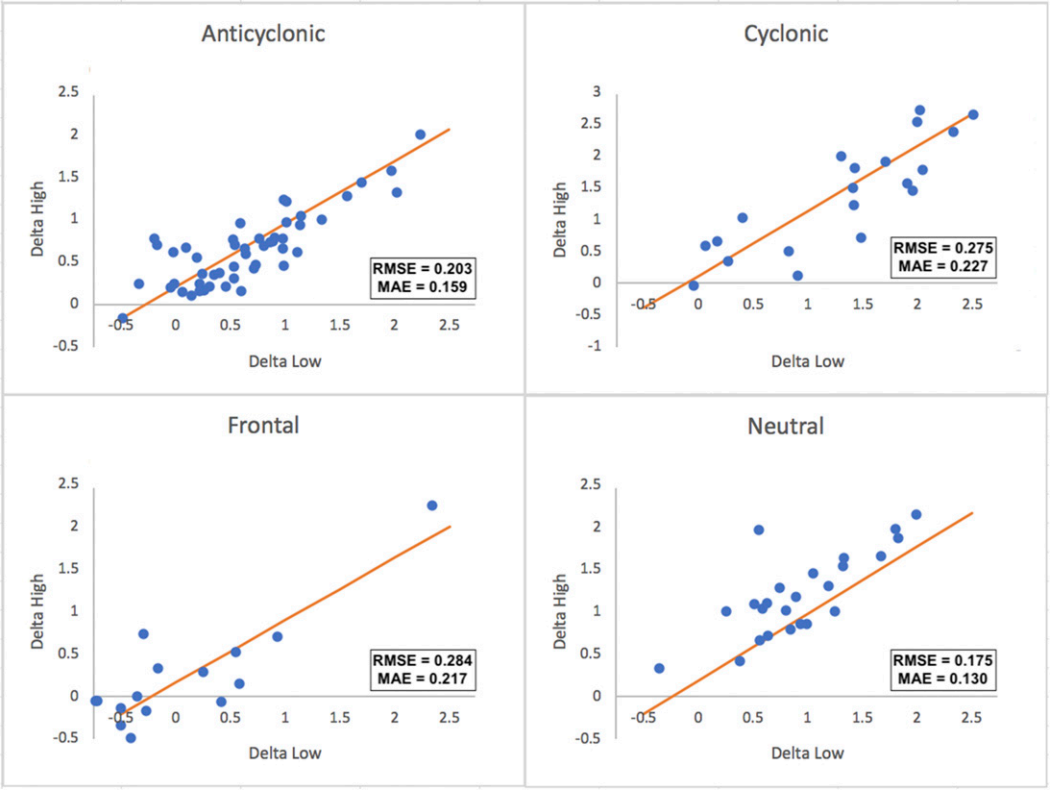

FIG. 9. 2018–19 flood event scatterplots of each category for delta high vs delta low. The trendline from the 1996–2014 models has been super imposed over each scatterplot. The RMSE and MAE values are indicated on the scatterplots.

TABLE 2. Values of astronomically predicted heights, predicted heights based on the statistical model described in the paper, and predicted heights based on the ETSS model (v2.2) are listed, as well as the verifying observations for the coastal flood event spanning 22–25 Nov 2018. The RMSE and MAE for the statistical model were 0.18 and 0.15, respectively, while the same values for the ETSS model were 0.28 and 0.23, respectively.

Date	Time (UTC)	Astronomically predicted height (ft MLLW)	Model-predicted height (ft MLLW)	ETSS forecast (ft MLLW)	Verified height (ft MLLW)	Model-predicted − verified	ETSS − verified
22 Nov 2018	1200	6.39	7.28	7.27	7.06	0.22	0.21
23 Nov 2018	0018	5.55	6.63	6.94	6.69	−0.06	0.25
23 Nov 2018	1300	6.58	8.09	8.33	8.14	−0.05	0.19
24 Nov 2018	0124	5.53	7.35	7.7	7.23	0.12	0.47
24 Nov 2018	1318	6.67	8.55	8.33	8.74	−0.19	−0.41
25 Nov 2018	0148	5.48	6.9	6.55	6.56	0.34	−0.01
25 Nov 2018	1406	6.66	7.72	7.74	7.68	0.04	0.06

regression-based approach, a comparison of the output from the NOAA extratropical storm surge (ETSS) model (Liu et al. 2019) was made. During 2018, NOAA/NWS was running version 2.2 of the ETSS model. Archived runs of the model were obtained for the time period of the case and predicted values from the model were compared to the output produced by the anticyclonic regression equation developed from the climatology (Table 2), based on the most recent run of the ETSS model available to forecasters at the time the regression model would be used by forecasters.

The regression-based model showed a slight improvement over ETSS in four of the seven tide cycles, while the ETSS showed a slight improvement in one of the seven tide cycles. For two of the cycles, the difference was negligible.

In all tide cycles during this extended event where the verified height reached above 7 ft MLLW, the difference between the prediction from the climatology method and the actual verifying height was 0.22 ft or less, all within the normal range of forecast for coastal water level at Charleston. RMSE and MAE were calculated for model predicted height and verified height as 0.18 and 0.15, respectively. The RMSE and MAE for the ETSS model test were 0.28 and 0.23, respectively.

6. Discussion

As the threat for coastal flooding in the Charleston area (and elsewhere) continues to rise, forecasts of expected levels of tidal inundation will need to continue improving. This climatological model method will be one tool that can aid the needed forecast improvement. Resulting in more accurate issuance of coastal flood advisories in Charleston, this allows for city officials to confidently communicate with the public about water levels and impacts such as road closures.

Forecasters will compare atmospheric model forecasts to the composite maps from this study and look for trends to determine the appropriate event type (cyclonic, anticyclonic, frontal, and neutral). Once the type is determined, the accompanying regression equation will enable forecasters to conclude a reasonably accurate assessment of maximum tidal levels approximately 6 h prior to the event, allowing for appropriate short-term mitigations.

The NWS, as part of the Weather-Ready Nation (WRN) initiative, is looking at expanding ways to communicate threats to the public and stakeholders so that both parties may receive actionable information in a timely manner (Uccellini and Ten Hoeve 2019). The current watch–warning–advisory (WWA) paradigm is in need of clarification and transition to provide additional information on creating visualizations and notification systems more pertinent to the user. These changes and expansions to NWS products and services are coming, but it is a slow process to meet all the requirements of federal regulations for change. However, to support any changes in NWS products and services, there needs to be a backbone of strong science that supports its utility in NWS forecast offices. This study is an example of that type of scientific effort (NWS 2019b).

Over the past half century, nuisance coastal flooding has caused gross damages and lost wages totaling over $1.53 billion (City of Charleston 2015). Flooding events disturb both the employees and the patrons of the city, and as these flooding events continue to become more common, so will the lost wages and the decrease of employee–patron interactions. Eventually a tipping point will be reached, and employees will no longer be able to sustain living in Charleston. Frequent coastal flooding events in Charleston could lead to a major economic downturn. An accurate nuisance coastal flood forecast with a 6-h lead time would help employees and employers make decisions on when and how to commute to work. Businesses can also take matters into their own hands by using the forecast to influence their own decisions regarding deliveries, supply chain, and physical protection.

7. Summary

Historical Charleston flood tide data from 1996 to 2014 can be used to provide CHS NWS forecasters with a climatology-based statistical tool to estimate total tide levels with each cycle, specifically related to levels that begin to cause impact and necessitate the issuance of coastal flood advisories. The potential for coastal flooding events to continue to increase by an order of magnitude as a result of sea level rise (IPCC 2013; Dahl et al. 2017) will make improved forecasting of coastal flooding imperative. And while nuisance floods do not always

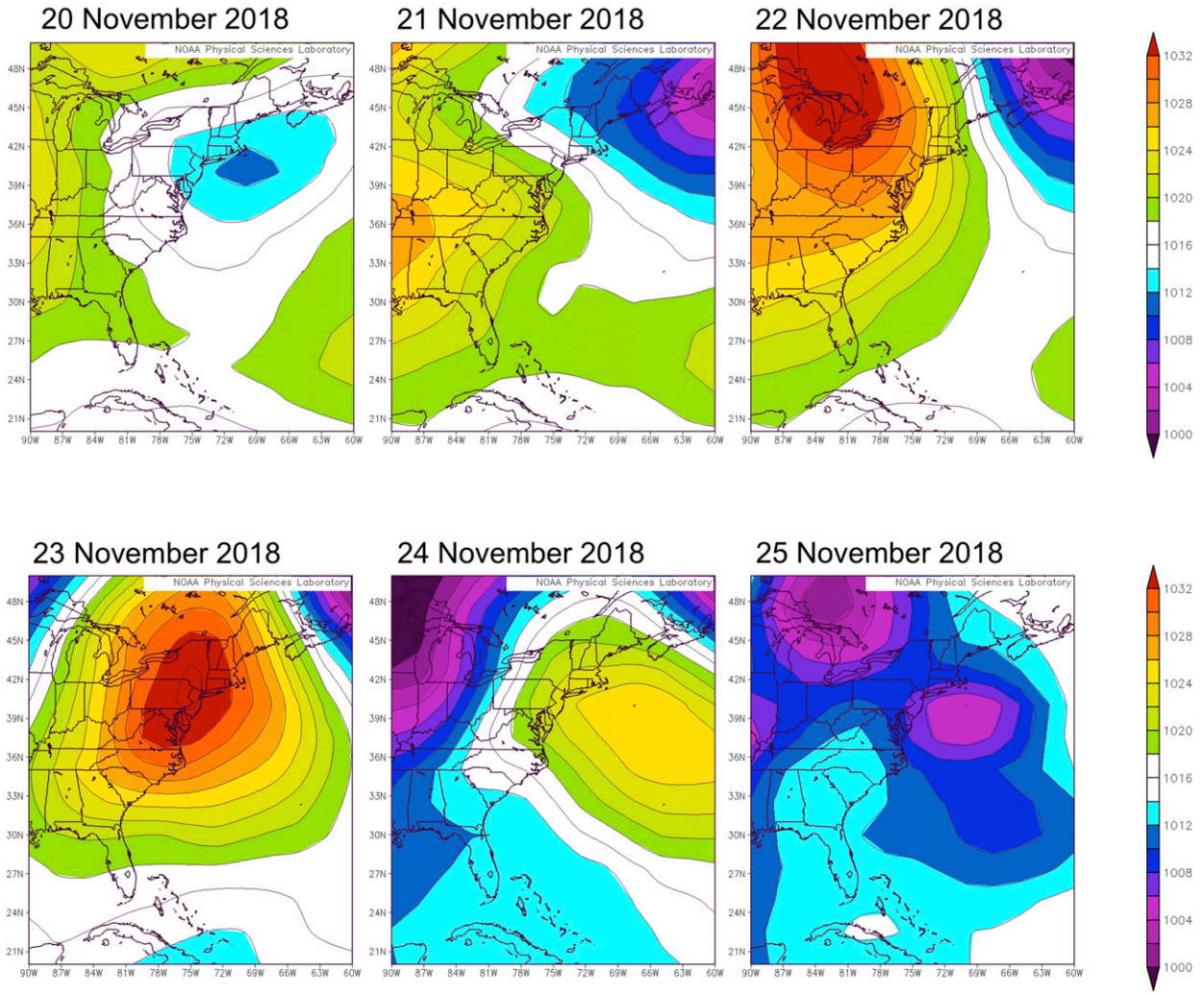

FIG. 10. NCEP–NCAR reanalysis maps of mean sea level pressure at the surface for 20–25 Nov 2018. Mean sea level pressures are measured in hectopascals.

pose an immediate risk to the community, their chronic occurrence can lead to negative infrastructural, socioeconomic, and health impacts (i.e., mold poisoning) (Curtis et al. 2004). Accurate forecasting must be applied in order to provide acute protection and mitigation in the short term.

Previous work has identified rapidly deepening cyclones, persistent onshore flow, and Ekman transport as drivers of nuisance flooding in the mid-Atlantic states but was unable to make definitive atmospheric correlations for nuisance flooding in Charleston and other coastal communities along the South Atlantic Bight (Sheridan et al. 2017). Approximately two-thirds of the events evaluated in this study fell into either the cyclonic or the anticyclonic category. The weather maps created for these two categories suggests that northeast wind anomalies off the coast of the northeastern and mid-Atlantic states could serve as an early warning signal for coastal flooding in South Carolina during the following days.

For the frontal cases, changes in pressure fields with time and how those changes impact wind can be used as signals to predict coastal flooding. If the changes in the pressure field promote winds having an easterly component off the coast of the southeastern and mid-Atlantic states, coastal flooding could occur as a result of wind water pushing toward the coast.

Neutral event flooding is more difficult to predict using atmospheric models because there are no strong weather indicators. Neutral event flooding and the outliers suggests that tide levels could be affected by factors that are not identified by the parameters used in this study.

Future work includes the development of a flood alert app where both flood levels and flood hazards such as road closures and power outages can be communicated to the public within a MLLW range using numbers and maps. To get the most accurate linear regression equations, the data analysis period for this study would need to be extended to current day. Coastal flooding events in Charleston during this last half decade have been exceedingly active (58 in 2015, 55 in 2016, 46 in 2017, 42 in 2018, and 89 in 2019). The equations would need to be updated yearly or biennially to capture the impacts of the most recent

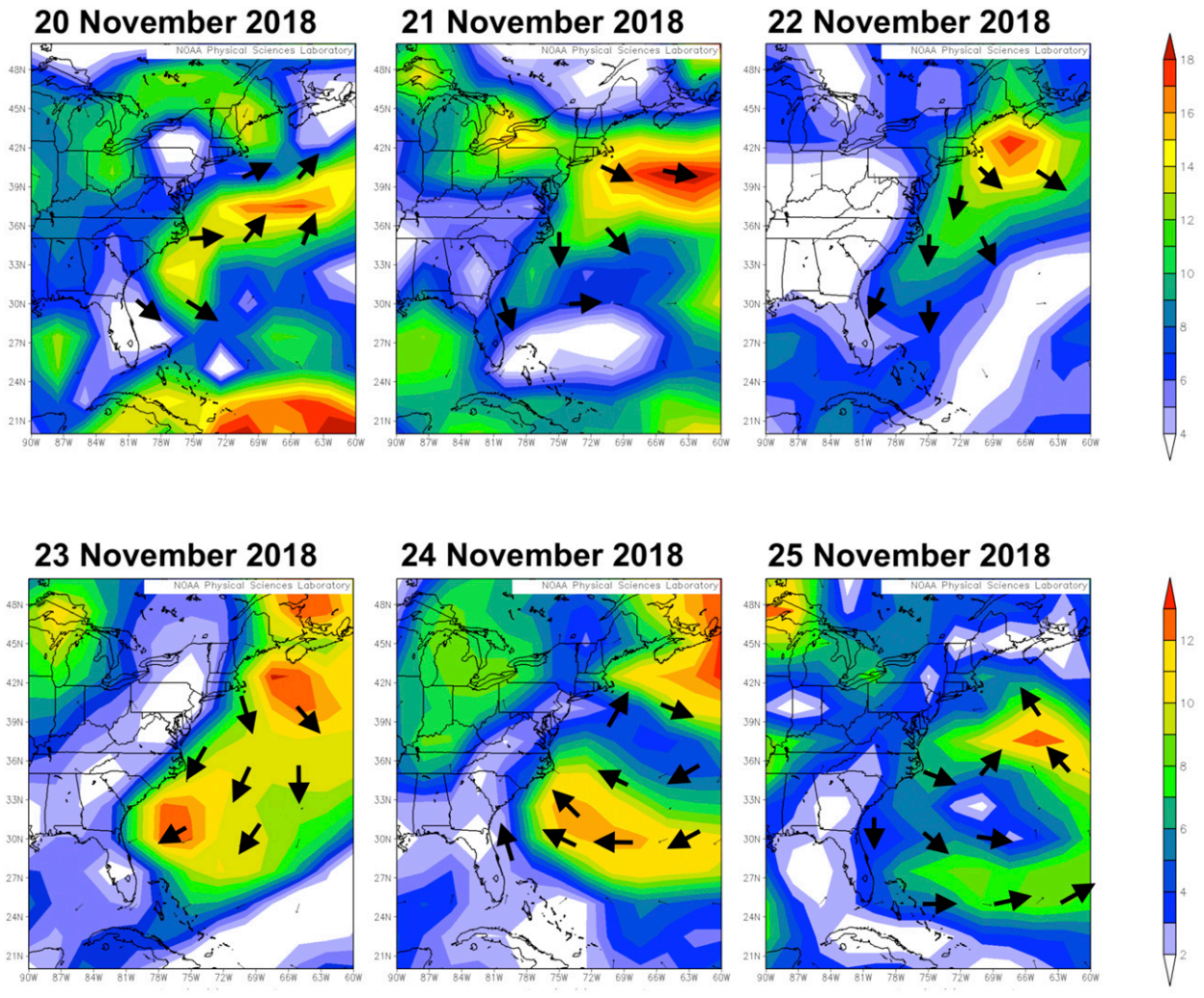

FIG. 11. NCEP–NCAR reanalysis maps of mean vector wind at the surface for 20–25 Nov 2018. Wind speed anomalies are measured in meters per second and the wind direction is indicated by the arrows.

events. The methodology presented in this study could be applied to other coastal communities so that they can create their own climatology-based forecast tools. Replicating this project for Fort Pulaski, Georgia, would be a good first step outside of Charleston. Further future work includes applying the weather type classifications to a longer time period and analyzing it for trends. The model should also be statistically analyzed against more independent data as it was during the November 2018 case study. It was observed that some of the outlier events in this study were influenced by distant large cyclones (tropical or extratropical). Examining nuisance flooding data for the contribution from distant tropical or extratropical cyclones is another potential area for future work. This study could also be used to influence work that is directed at predicting the starting and ending times of nuisance coastal flooding events.

Acknowledgments. Dan Burger and Matthew Nowlin are thanked for substantial contributions in the areas of tool application and public policy, respectively. The authors appreciate the efforts of the staff that maintain the NOAA Tides and Currents website, from which the data used in this project were obtained. The authors also thank the staff from the NOAA ESRL that maintain the NCEP–NCAR reanalysis data composite database, from which the data used in this project were obtained. The NWS CHS WFO staff is thanked for their assistance with gathering the data displayed in Fig. 2. Finally, the authors thank the staff from the NOAA NHC that maintain the past track seasonal map archives that were used in this project.

This manuscript was prepared under Subaward Z16-23457 with the University Corporation for Atmospheric Research (UCAR) under Cooperative Agreement NA11NWS4670004 with the National Oceanic and Atmospheric Administration (NOAA), U.S. Department of Commerce (DoC). The statements, findings, conclusions, and recommendations are those of the authors and do not necessarily reflect the views of NOAA, DoC, or UCAR.

Data availability statement. All historical 6-min tidal data created or used during this study are openly available from the NOAA Tides and Current's Water Level Reports (Station 8665530) at https://tidesandcurrents.noaa.gov/reports.html?id=8665530. All 6-h NCEP–NCAR reanalysis data composite maps created or used during this study are openly available from NOAA's Physical Sciences Laboratory at https://psl.noaa.gov/data/composites/hour/. All the daily mean composite maps created or used during this study are openly available from the NOAA's Physical Sciences Laboratory at https://psl.noaa.gov/data/composites/day/. The data used to create Fig. 2 in this study are openly available from the NWS's Coastal Flood Event Data Base for Charleston at https://www.weather.gov/chs/coastalflood.

REFERENCES

Adger, W. N., T. P. Hughes, C. Folke, S. R. Carpenter, and J. Rockström, 2005: Social-ecological resilience to coastal disasters. *Science*, **309**, 1036–1039, https://doi.org/10.1126/science.1112122.

Alsheimer, F., and B. L. Lindner, 2011: Synoptic-scale precursors to high-impact weather events in the Georgia and South Carolina coastal region. *J. Coastal Res.*, **272**, 263–275, https://doi.org/10.2112/JCOASTRES-D-10-00048.1.

Behre, R., 2017: Raising Charleston's low battery expected to cost $100 million and take a decade or more to complete. *Post and Courier*, 15 July, http://www.postandcourier.com/news/raising-charleston-s-low-battery-expected-to-cost-million-and/article_e6b95248-6747-11e7-8ee7-1f03feedbb40.html.

——, and A. Darlington, 2017: Charleston's 34-year-old list of drainage projects not quite half done after $239 million. *Post and Courier*, 9 September, https://www.postandcourier.com/news/charleston-s–year-old-list-of-drainage-projects-not/article_77a09ea0-9278-11e7-aba2-6f65d7bc0420.html.

Charleston County Government, 2021: Emergency operations plan. Charleston County, South Carolina, 330 pp, https://www.charlestoncounty.org/departments/emergency-management/files/EOP.pdf.

Church, J. A., and N. J. White, 2011: Sea-level rise from the late 19th to the early 21st century. *Surv. Geophys.*, **32**, 585–602, https://doi.org/10.1007/s10712-011-9119-1.

City of Charleston, 2015: Sea level rise strategy. City of Charleston, South Carolina, 20 pp., accessed 12 March 2017, https://www.charleston-sc.gov/DocumentCenter/View/10089/12_21_15_Sea-Level-Strategy_v2_reduce?bidId=.

——, 2019a: Flooding and sea level rise strategy. City of Charleston, South Carolina, 20 pp., accessed 18 February 2020, https://www.charleston-sc.gov/DocumentCenter/View/20299/Flooding-and-Sea-Level-Rise-Strategy-2019-web-viewing?bidId=.

——, 2019b: FloodStat meeting report. City of Charleston, South Carolina, 17 pp., https://www.charleston-sc.gov/DocumentCenter/View/25746/FloodStat_201911_MeetingReport.

Colle, B. A., K. Rojowsky, and F. Buonaito, 2010: New York City storm surges: Climatology and an analysis of the wind and cyclone evolution. *J. Appl. Meteor. Climatol.*, **49**, 85–100, https://doi.org/10.1175/2009JAMC2189.1.

Curtis, M. S., A. Lieberman, M. Stark, W. Rea, and M. Vetter, 2004: Adverse health effects of indoor molds. *J. Nutr. Environ. Med.*, **14**, 261–274, https://doi.org/10.1080/13590840400010318.

Dahl, K. A., M. F. Fitzpatrick, and E. Spanger-Siegfried, 2017: Sea level rise drives increased tidal flooding frequency at tide gauges along the U.S. East and Gulf Coasts: Projections for 2030 and 2045. *PLOS ONE*, **12**, 1–24, https://doi.org/10.1371/journal.pone.0170949.

Gornitz, V. M., R. C. Daniels, T. W. White, and K. R. Birdwell, 1994: The development of a coastal risk assessment database: Vulnerability to sea-level rise in the U.S. Southeast. *J. Coastal Res.*, **12**, 327–338.

——, S. Couch, and E. K. Hartig, 2001: Impacts of sea level rise in the New York City metropolitan area. *Global Planet. Change*, **32**, 61–88, https://doi.org/10.1016/S0921-8181(01)00150-3.

Hebert, P. J., 1980: Atlantic hurricane season of 1979. *Mon. Wea. Rev.*, **108**, 973–990, https://doi.org/10.1175/1520-0493(1980)108<0973:AHSO>2.0.CO;2.

IPCC, 2013: Summary for policymakers. *Climate Change 2013: The Physical Science Basis*, T. F. Stocker et al., Eds., Cambridge University Press, 1–29.

Kriebel, D. L., and J. D. Geiman, 2014: A coastal flood stage to define existing and future sea-level hazards. *J. Coast. Res.*, **30**, 1017–1024, https://doi.org/10.2112/JCOASTRES-D-13-00068.1.

Landsea, C. W., and J. L. Franklin, 2013: Atlantic hurricane database uncertainty and presentation of a new database format. *Mon. Wea. Rev.*, **141**, 3576–3592, https://doi.org/10.1175/MWR-D-12-00254.1.

Lindner, B. L., and A. Neuhauser, 2018: Climatology and variability of tropical cyclones affecting Charleston, South Carolina. *J. Coastal Res.*, **34**, 1052–1064, https://doi.org/10.2112/JCOASTRES-D-17-00135.1.

Lindsey, R., 2020: Climate change: Global sea level. NOAA, accessed 9 June 2018, https://www.climate.gov/news-features/understanding-climate/climate-change-global-sea-level.

Liu, H., A. Taylor, and K. Kang, 2019: Latest development in the NWS' extra-tropical storm surge model and probabilistic extra-tropical storm surge model. *17th Symp. on the Coastal Environment*, Phoenix, AZ, Amer. Meteor. Soc., 3.8, https://ams.confex.com/ams/2019Annual/mediafile/Manuscript/Paper355246/AMS_abstract_extend.pdf.

McLean, R., A. Tsyban, V. Burkett, J. O. Codignotto, D. L. Forbes, N. Mimura, R. J. Beamish, and V. Ittekkot, 2001: Coastal zone and marine ecosystems. *Climate Change 2001: Impacts, Adaptation and Vulnerability*, J. J. McCarthy et al., Eds., Cambridge University Press, 343–390.

Moftakhari, H. R., A. AghaKouchak, B. F. Sanders, D. L. Feldman, W. Sweet, R. A. Matthew, and A. Luke, 2015: Increased nuisance flooding due to sea-level rise: Past and future. *Geophys. Res. Lett.*, **42**, 9846–9852, https://doi.org/10.1002/2015GL066072.

Nicholls, R. J., 2004: Coastal flooding and wetland loss in the 21st century: Changes under the SRES climate and socio-economic scenarios. *Global Environ. Change*, **14**, 69–86, https://doi.org/10.1016/j.gloenvcha.2003.10.007.

——, and A. Cazenave, 2010: Sea-level rise and its impact on coastal zones. *Science*, **328**, 1517–1520, https://doi.org/10.1126/science.1185782.

NOAA, 2018: Daily weather maps: EV2—Daily weather map. NCEI, accessed 27 March 2020, https://www.ncei.noaa.gov/access/metadata/landing-page/bin/iso?id=gov.noaa.ncdc:C01006.

——, 2020a: Tides and currents: Tidal datums. Center for Operational Oceanographic Products and Services, accessed 20 April 2020, https://tidesandcurrents.noaa.gov/datum_options.html.

——, 2020b: Tides and currents: Water level reports. Accessed 10 January 2020, https://tidesandcurrents.noaa.gov/reports.html?id=8665530.

NWS, 2016: Service assessment: The historic South Carolina floods of October 1–5, 2015. NOAA, 113 pp., accessed 22 October 2020, https://www.weather.gov/media/publications/assessments/SCFlooding_072216_Signed_Final.pdf.

——, 2018: National weather service eastern region supplement 01-2018: Coastal flood categories. NOAA, 9 pp., accessed 24 September 2020, https://www.nws.noaa.gov/directives/sym/pd01001003a012018curr.pdf.

——, 2019a: Advanced hydrologic prediction service. NOAA, accessed 29 March 2020, https://water.weather.gov/ahps2/hydrograph.php?gage=chts1&wfo=chs.

——, 2019b: Weather-Ready Nation. NOAA, accessed 20 November 2019, https://www.weather.gov/wrn/.

——, 2020: National Weather Service instruction 10-320: Surf zone forecast and coastal/lakeshore hazard services. NOAA, 38 pp., accessed 16 September 2020, https://www.nws.noaa.gov/directives/sym/pd01003020curr.pdf.

Sheridan, S. C., D. E. Pirhalla, C. C. Lee, and V. Ransibrahmanakul, 2017: Atmospheric drivers of the sea-level fluctuations and nuisance floods along the mid-Atlantic coast of the USA. *Reg. Environ. Change*, **17**, 1853–1861, https://doi.org/10.1007/s10113-017-1156-y.

Slade, D., 2017: Why heavy rain brings the Charleston area to a standstill, and what's being done. *Post and Courier*, 25 April, http://www.postandcourier.com/news/why-heavy-rain-brings-the-charleston-area-to-a-standstill/article_8223564e-2903-11e7-851d-573201fe8b62.html.

Smith, K., and R. Ward, 1998: *Floods: Physical Processes and Human Impacts*. Wiley, 382 pp.

Spanger-Siegfried, E., M. Fitzpatrick, and K. Dahl, 2014: Encroaching tides: How sea level rise and tidal flooding threaten U.S. East and Gulf Coast communities over the next 30 years. Union of Concerned Scientists, 76 pp., https://www.ucsusa.org/sites/default/files/attach/2014/10/encroaching-tides-full-report.pdf.

Sverdrup, H. U., M. W. Johnson, and R. H. Fleming, 1942: *The Oceans: Their Physics, Chemistry, and Biology*. Prentice Hall, 1087 pp.

Sweet, W. V., C. Zervas, and S. Gill, 2009: Elevated East Coast sea level anomaly: June–July 2009. NOAA Tech. Rep. NOS CO-OPS 051, 40 pp., https://beta.tidesandcurrents.noaa.gov/publications/EastCoastSeaLevelAnomaly_2009.pdf.

——, J. Park, J. J. Marra, C. Zervas, and S. Gill, 2014: Sea level rise and nuisance flood frequency changes around the United States. NOAA Tech. Rep. NOS COOPS 73, 53 pp., https://tidesandcurrents.noaa.gov/publications/NOAA_Technical_Report_NOS_COOPS_073.pdf.

Uccellini, L. W., and J. E. Ten Hoeve, 2019: Evolving the national weather service to build a Weather-Ready Nation: Connecting observations, forecasts, and warnings to decision-makers through impact-based decision support services. *Bull. Amer. Meteor. Soc.*, **100**, 1923–1942, https://doi.org/10.1175/BAMS-D-18-0159.1.

Walsh, J., and Coauthors, 2014: Our changing climate. *Climate Change Impacts in the United States: The Third National Climate Assessment*, J. M. Melillo, T. C. Richmond, and G. W. Yohe, Eds., U.S. Global Change Research Program Rep., 19–67, https://doi.org/10.7930/J0KW5CXT.

Wolf, J., 2009: Coastal flooding: Impacts of coupled wave-surge-tide models. *Nat. Hazards*, **49**, 241–260, https://doi.org/10.1007/s11069-008-9316-5.

Woodworth, P. L., M. Maqueda, M. A. Roussenov, V. M. Williams, and R. G. Hughes, 2014: Mean sea level variability along the northeast American Atlantic coast, and the roles of the wind and the overturning circulation. *J. Geophys. Res. Oceans*, **119**, 8916–8935, https://doi.org/10.1002/2014JC010520.

Yin, J., S. M. Griffies, M. Winton, M. Zhao, and L. Zanna, 2020: Response of storm-related extreme sea level along the U.S. Atlantic coast to combine weather and climate forcing. *J. Climate*, **33**, 3745–3769, https://doi.org/10.1175/JCLI-D-19-0551.1.